


# Creation mechanism of electron-positron pair on equally spaced multiple localized fields

Chuan-Ke Li(李传可), Nan-Sheng Lin(林南省), Xian-Xian Zhou(周鲜鲜), Miao Jiang(江淼), and Ying-Jun Li(李英骏)

**Citation:**Chin. Phys. B, 2023, 32 (**9**): 094202. DOI: 10.1088/1674-1056/acd7cd
Journal homepage: http://cpb.iphy.ac.cn; http://iopscience.iop.org/cpb

**What follows is a list of articles you may be interested in**

---

## Microwave absorption and bandwidth study of $Y_2Co_{17}$ rare earth soft magnetic alloy with easy-plane anisotropy

Yun-Guo Ma(马云国), Liang Qiao(乔亮), Zu-Ying Zheng(郑祖应), Hong-Bo Hao(郝宏波), Hao Wang(王浩), Zhe Sun(孙哲), Cheng-Fa Tu(涂成发), Tao Wang(王涛), Zheng Yang(杨正), and Fa-Shen Li(李发伸)

Chin. Phys. B, 2023, 32 (**8**): 084202. DOI: 10.1088/1674-1056/aca148

## High-performance chiral all-optical OR logic gate based on topological edge states of valley photonic crystal

Xiaorong Wang(王晓蓉), Hongming Fei(费宏明), Han Lin(林瀚), Min Wu(武敏), Lijuan Kang(康丽娟), Mingda Zhang(张明达), Xin Liu(刘欣), Yibiao Yang(杨毅彪), and Liantuan Xiao(肖连团)

Chin. Phys. B, 2023, 32 (**7**): 074205. DOI: 10.1088/1674-1056/accb41

## High efficiency and high transmission asymmetric polarization converter with chiral metasurface in visible and near-infrared region

Yuhang Gao(高雨航), Yu Tian(田宇), Qingguo Du(杜庆国), Yuanli Wang(王原丽), Qin Fu(付琴), Qiang Bian(卞强), Zhengying Li(李政颖), Shuai Feng(冯帅), and Fangfang Ren(任芳芳)

Chin. Phys. B, 2023, 32 (**7**): 074201. DOI: 10.1088/1674-1056/acb9eb

## Theoretical research on the transverse spin of structured optical fields inside a waveguide

Zhiyong Wang(王智勇), Xiangru Wang(汪相如), Anran Li(李岸然), Kaiqiang Zhang(张开强), Yukun Ji(纪玉坤), and Mingyu Zhong(钟明玉)

Chin. Phys. B, 2023, 32 (**6**): 064207. DOI: 10.1088/1674-1056/acbf28

## Optically pumped wavelength-tunable lasing from a GaN beam cavity with an integrated Joule heater pivoted on Si

Feifei Qin(秦飞飞), Yang Sun(孙阳), Ying Yang(杨颖), Xin Li(李欣), Xu Wang(王旭), Junfeng Lu(卢俊峰), Yongjin Wang(王永进), and Gangyi Zhu(朱刚毅)

Chin. Phys. B, 2023, 32 (**5**): 054210. DOI: 10.1088/1674-1056/acc05e

---

# Creation mechanism of electron–positron pair on equally spaced multiple localized fields

Chuan-Ke Li(李传可)[1], Nan-Sheng Lin(林南省)[2,†], Xian-Xian Zhou(周鲜鲜)[3], Miao Jiang(江淼)[2], and Ying-Jun Li(李英骏)[1,2,‡]

[1] *State Key Laboratory for GeoMechanics and Deep Underground Engineering, China University of Mining and Technology, Beijing* 100083, *China*
[2] *School of Science, China University of Mining and Technology, Beijing* 100083, *China*
[3] *School of Management Science and Engineering, Anhui University of Finance and Economics, Bengbu* 233030, *China*

(Received 22 February 2023; revised manuscript received 27 April 2023; accepted manuscript online 23 May 2023)

We investigate the electron–positron creation process from multiple equally spaced distributed oscillating electric fields. The computational quantum field theory (CQFT) is applied to analyze the effect of the number of local fields, the distance between them, and their potential height on the created particle number. It is found that whether adjacent electric fields overlap plays an important role. The creation rate exhibits a direct linear relationship with the number of fields when they do not overlap, but exceeds the sum of the rate when the fields alone. They exhibit a distinctly nonlinear relationship when they overlap, and in particular exhibit a quadratic relationship when the fields completely overlap. These phenomena corroborate that the particle pair creation in the interaction region is non-uniform and influenced by the strength of the central strongest electric field.

**Keywords:** electron-positron pair creation, ultra-strong laser field, computational quantum field theory

**PACS:** 42.25.Bs, 03.65.–w, 12.20.–m **DOI:** 10.1088/1674-1056/acd7cd

## 1. Introduction

Pair creation from the vacuum is a phenomenon where a vacuum in the presence of a supercritical electromagnetic field is unstable and decays into electron–positron pairs.[1,2] It may be the most intriguing prediction of quantum electrodynamics (QED) and has been studied with different methods since Dirac put forward the relativistic wave equation and predicted the existence of positrons.[3] In the 1930s, the pioneering research of the electron–positron pair creation induced by the ultra-strong field was engaged by Sauter,[4] Heisenberg and Euler.[5] Schwinger[6] formalized the pair creation process in the language of QED and recovered the pair creation rate in a constant electric field with the proper-time method, so sometimes the tunneling pair creation is also called the Schwinger pair creation or the Schwinger effect. Brezin and Itzykson[7] extended the research to the vacuum pair creation in a time-dependent electric field with the Wentzel–Kramers–Brillouin (WKB) approximation and found the multi-photon pair creation process, which was different from the Schwinger tunneling process. Moreover, various methods are widely utilized in this field, such as the world-line instantons technique,[8–12] quantum kinetic theory, which includes the quantum Vlasov equation (QVE)[13–19] and real-time Dirac–Heisenberg–Wigner (DHW) formalism,[20–27] as well as computational quantum field theory (CQFT).[28–46] Recently, the relation between these methods has been explored. Dumlu[47] proved that the QVE is equivalent to the semiclassical scattering method in both scalar QED and spinor QED. Hebenstreit *et al.*[20] found that the Wigner function in spinor QED could be reduced to the QVE for a uniform and time-varying electric field with one component. Li *et al.*[27] generalized the above result to the scalar QED, and found that in this case the electric field could have three components. Li *et al.*[48] demonstrated theoretically that the CQFT is equivalent to the quantum kinetic theory for pair creation in a space-independent and time-inhomogeneous electric field.

The optical intensity in the focal region can be enhanced considerably by the tight focusing.[49,50] In 2021, Jin *et al.*[50] realized ultra-high intensity over $10^{23}$ W/cm$^2$ by tightly focusing the CoReLS petaWatt (PW) laser. More exciting achievement is the ultra-high intensity and ultra-short laser facilities under construction, such as the Extreme Light Infrastructure (ELI)[51] in European, whose intensity is expected to be $10^{24}$–$10^{26}$ W/cm$^2$. However, the critical field strength to generate a significant amount of pairs was estimated to be on the order of $10^{29}$ W/cm$^2$, which is stronger than these laser facilities by several orders of magnitude.[6] Partly motivated by these difficulties, Schützhold *et al.* proposed a dynamically assisted Schwinger mechanism,[10] by combination of a strong and slowly varying electric field and a weak and rapidly changing electromagnetic field. The dynamically assisted Schwinger mechanism shows a possibility to enhance the pair creation rate significantly and results in a decrease of the effective spectral gap between the positive continuous state and the Dirac

†Corresponding author. E-mail: phy.nslin@gmail.com
‡Corresponding author. E-mail: lyj@aphy.iphy.ac.cn

© 2023 Chinese Physical Society and IOP Publishing Ltd 

sea. The scheme of simultaneous multiple pulses focusing on one spot from the structural features of the ELI facility has been proposed.[52–55] The field configuration leads to a significant reduction of the threshold energy needed for the pair creation to become observable compared to the case of one pulse. Su *et al.* designed a multifield configuration by applying several localized subcritical static electric fields side by side and lowered the threshold of pair creation with quantum tunneling.[30,34]

In this paper, we explore the process of electron–positron pair creation in the presence of multiple electric fields that vary in space and time. Specifically, we investigate the impact of the number of electric fields, their spatial separation, and their potential height on the probability of pair creation. Our findings offer valuable insights into the visualization and understanding of pair creation in multiple fields. Ultimately, this research provides theoretical reference for experiments of vacuum pair creation detection.

This paper is organized as follows. In order to render the presentation self-contained, Section 2 is devoted to a concise review of the theoretical framework of the computational quantum field theory. In Section 3, the electron–positron pair creation induced by multiple localized fields is investigated, and the results are discussed. In Section 4, we give our conclusions.

## 2. The theoretical framework of computational quantum field theory

To study the electron–positron pair creation process, the quantum field theory is necessary to understand the particle creation and annihilation. We introduce a time-dependent field operator $\hat{\psi}(t)$ and the Hamiltonian of quantum field theory $\hat{H}$ to describe creation and annihilation processes. They obey the Heisenberg equation of motion, $\mathrm{i}\partial\hat{\psi}(t)/\partial t = [\hat{H},\hat{\psi}(t)]$. However, we neglect the interfermionic interaction and treat external fields as classical in strong field approximation. Then, the Heisenberg equation is equivalent to the Dirac equation[28,56]

$$\mathrm{i}\partial\hat{\psi}(t)/\partial t = [c\sigma_1 p + \sigma_3 c^2 + V(z,t)]\hat{\psi}(t). \tag{1}$$

Here, $c$ is the speed of light in vacuum, $\sigma_1$ and $\sigma_3$ are the Pauli matrices. The electric field is described by the scalar potential $V(z,t)$. In this paper we use atomic units, so $c = 137.036$ a.u.. The four-component Dirac spinor wave functions can be reduced to two components when the electric field is homogeneous in both the $x$ and $y$ directions.[28] The field operator $\hat{\psi}(z,t)$ can be expanded by field-free energy eigenstates $u_p(z)$ $(E \geq c^2)$ and $u_n(z)$ $(E \leq -c^2)$ as

$$\begin{aligned}\hat{\psi}(z,t) &= \sum_p \hat{b}_p(t)u_p(z) + \sum_n \hat{d}_n^{\dagger}(t)u_n(z)\\ &= \sum_p \hat{b}_p u_p(z,t) + \sum_n \hat{d}_n^{\dagger}u_n(z,t),\end{aligned} \tag{2}$$

where $\hat{b}_p$ and $\hat{d}_n^{\dagger}$ are the particle annihilation and the antiparticle creation operators, respectively; the subscripts $p$ ($n$) represent positive (negative) energy; $u_p(z,t)$ and $u_n(z,t)$ are time-dependent wavefunction. The time-dependent operators of fermion creation and annihilation are

$$\hat{b}_p(t) = \sum_{p'}\hat{b}_{p'}\int \mathrm{d}z u_p^*(z)u_{p'}(z,t) + \sum_{n'}\hat{d}_{n'}^{\dagger}\int \mathrm{d}z u_p^*(z)u_{n'}(z,t), \tag{3}$$

$$\hat{d}_n^{\dagger}(t) = \sum_{p'}\hat{b}_{p'}\int \mathrm{d}z u_n^*(z)u_{p'}(z,t) + \sum_{n'}\hat{d}_{n'}^{\dagger}\int \mathrm{d}z u_n^*(z)u_{n'}(z,t). \tag{4}$$

The electronic portion is defined as $\hat{\psi}^{(\mathrm{e})}(z,t) = \sum_p \hat{b}_p(t)u_p(z)$. Then the spatial number density of electrons reads

$$\begin{aligned}\rho(z,t) &= \langle\!\langle \mathrm{vac} \parallel \hat{\psi}^{(\mathrm{e})\dagger}(z,t)\hat{\psi}^{(\mathrm{e})}(z,t) \parallel \mathrm{vac}\rangle\!\rangle\\ &= \sum_n \Big|\sum_p \boldsymbol{U}_{p,n}(t)u_p(z)\Big|^2,\end{aligned} \tag{5}$$

and the momentum distribution reads

$$\rho(p,t) = \sum_n |\boldsymbol{U}_{p,n}(t)|^2, \tag{6}$$

where $\boldsymbol{U}_{p,n}(t) = \int \mathrm{d}z u_p^*(z)u_n(z,t)$ is a time evolution matrix. The state $u_n(z,t)$ can be obtained by applying the split-operator method to evolve initial field-free eigenstate $u_n(z)$ under the interaction, and then is projected onto $u_p(z)$; $\|\mathrm{vac}\rangle\!\rangle$ is the Fock representation of the field-free vacuum, and $\rho(z,t)$ represents the spatial density of real electrons. Its trace $\mathrm{tr}[\rho(z,t)]$ represents the total number of created pairs, so

$$N(t) = \int \mathrm{d}z\rho(z,t) = \sum_{p,n}|U_{p,n}(t)|^2. \tag{7}$$

## 3. Numerical simulations and results

In the following, we consider several electric fields of the colliding laser pulses whose temporal and spatial variations are independent. Because the electric field is homogeneous in $x$ and $y$ directions, the electric field can be represented by the scalar potential

$$V(z,t) = \sum_{i=1}^{M} V_i(z)f(t)\theta(t), \tag{8}$$

where $M$ is the number of fields, $V_i(z)$ and $f(t)\theta(t)$ describe the spatial and temporal variations of the electric field, respectively. The spatial profile of the field is a Sauter potential acting along the $z$ direction

$$V_i(z) = \frac{V_0}{2}\left\{1 + \tanh\left[(z - z_0 - (i-1)d)/W_0\right]\right\}, \tag{9}$$

where $V_0$ is the height of fields, $W_0$ is characteristic width, $z_0$ is the center of fields, and $d$ is the distance of the adjacent field

center. Typical configurations of the multiple fields are shown in Fig. 1.

The temporal component includes two parts: a long-term oscillation

$$f(t) = \sin(\omega t), \tag{10}$$

where $\omega$ is the frequency of the laser pulses, and a turn-on function

$$\theta(t) = \begin{cases} \sin^2(\pi t/2T), & 0 \le t \le T, \\ 1, & T < t, \end{cases} \tag{11}$$

where $T = 2\pi/\omega$ is one laser period. In the numerical implementation, the scalar potential (the multiple Sauter potential, see Eq. (9)) is modified by a pulse shape function consisting of $\sin^2$ turn-on, and followed by a plateau region to avoid drastically switching on in time.

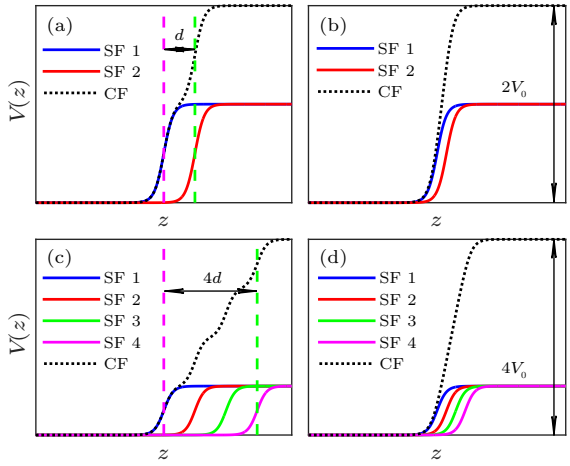



**Fig. 1.** Schematic of the multiple fields for different distance $d$ and fields number $M$: (a) a non-overlap field between two fields, (b) an overlap field between two fields, (c) a non-overlap field among four fields, and (d) an overlap field among four fields. The solid line represents a single field (SF), and the dotted line represents a combined field (CF).

### 3.1. Pair creation in the multiple equidistant fields

In this section, we study the electron–positron pair creation induced by multiple equidistant fields, as shown in Fig. 1. The electron–positron pairs are created continuously at a constant rate for the reason that $\omega = 2.5c^2 > 2c^2$ (shown in Fig. 2). Because the combined field strength is enhanced with increasing the number of fields, the created pair number grows significantly.

To enable a comparison of particle pair creation induced by multiple fields at different distances, we calculate the resulting number of pairs $n_M$ at 20 laser period, which is presented in Table 1. When the multiple electric fields completely overlap ($d = 0$), the total strength of $M$ laser fields is $M$ times of a single field, i.e., $E_M = ME_1$. Brezin and Itzykson used the Wentzel–Kramers–Brillouin (WKB) approximation to analyze the creation of positron-electron pairs through multi-photon absorption processes, and also found that the creation rate $\Gamma$ is directly proportional to the square of the field strength.[7] It is reasonable that the particle pairs created by the oscillating field are quadratically related to the total field strength when $d = 0$. However, it is under a different scenario when the multiple fields are well separated ($d \ge W_0$). We have found that the number of total pairs, $n_M$, depends linearly on $n_1$. The slope of function $n_M(M)$ is reduced significantly by increasing the distance $d$. For instance, the linear relationships are $n_M = 0.0548(M-1)+n_1$, $n_M = 0.032(M-1)+n_1$, and $n_M = 0.02457(M-1)+n_1$ for the distances $d = W_0$, $2W_0$, and $3W_0$, respectively. The linear relationship between the pair creation in multiple fields and a single field is weakened as the distance $d$ increases. The creation of pairs in the multiple fields becomes mutually influenced in space when the distance between the fields is greater than the characteristic width $W_0$. Although the effect weakens as the distance between the fields increases, the presence of other fields continues to impact the pair creation process of each field. The energy distribution of the pairs exhibits oscillatory behavior, which is due to the interference of the created particles from localized fields.[32] As the distance $d$ approaches infinity, the energy distribution becomes much wider and only exhibits a single peak at $E = \omega/2$ due to the symmetry, and the total number $n_M$ approaches $Mn_1$.

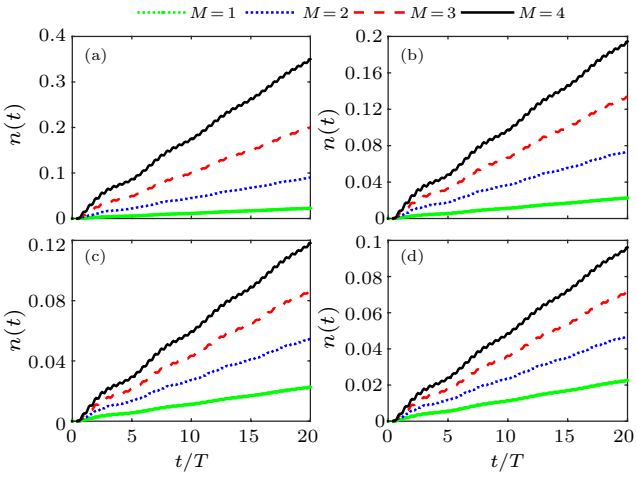



**Fig. 2.** Evolving number of the electron–positron pairs for the different distance between fields: (a) $d = 0$, (b) $W_0$, (c) $2W_0$, and (d) $3W_0$. The green dot-dashed line, the blue dotted line, the red dashed line and the black solid line represent $M = 1$, 2, 3 and 4, respectively. Here, $V_0 = 0.3c^2$, $W_0 = 3/c$, and $\omega = 2.5c^2$. The time is in units of the laser period $T = 2\pi/\omega$.

**Table 1.** The number of created pairs at 20 laser periods for different distance between fields $d$ and fields number $M$.

| $d$ | $M=1$ | $M=2$ | $M=3$ | $M=4$ |
|---|---|---|---|---|
| 0 | 0.02264 | 0.08996 | 0.20011 | 0.35021 |
| $W_0$ | 0.02264 | 0.07408 | 0.13402 | 0.19451 |
| $2W_0$ | 0.02264 | 0.05471 | 0.08673 | 0.11826 |
| $3W_0$ | 0.02264 | 0.04731 | 0.07176 | 0.09612 |

In our model, the height of the electric potential corresponds to the oscillating field's amplitude. There is a corresponding increase in the number of pairs created as the height of the electric potential increases, as shown in Fig. 3. We increase the original potential height $V_0$ by factors of 1.6 and

2 from $0.3c^2$ to $0.48c^2$ and $0.6c^2$. The field strength is determined by the spatial derivative of the scalar potential ($E(z,t) = \partial V(z,t)/\partial z$), and it leads to the strength $E_0 = V_0/2W_0$, where $2W_0$ is the effective field width. The electric field strength $E$ is proportional to the height $V_0$ when $W_0$ stays the same. According to the relationship $\Gamma \propto E^2$, the creation rates have increased up to 2.56 times and 4 times, respectively. This means that the rate of pair creation has significantly increased with the increment of the electric field strength. Figure 3(a) presents the number of pairs created by a single field, with creation rates shown for potential heights of $0.3c^2$ (8.41 a.u.), $0.48c^2$ (21.45 a.u.), and $0.6c^2$ (33.40 a.u.). The creation rates of electron–positron pairs for two fields are listed in Table 2. These results show that the creation rate is directly proportional to the square of the field strength.

**Table 2.** The creation rates of electron–positron pairs for different distances between fields $d$.

| $V_0$ | $d=0, M=2$ | $d=W_0, M=2$ | $d=2W_0, M=2$ |
|---|---|---|---|
| $0.3c^2$ | 33.40 a.u. | 27.62 a.u. | 20.37 a.u. |
| $0.48c^2$ | 84.27 a.u. | 69.74 a.u. | 51.47 a.u. |
| $0.6c^2$ | 129.95 a.u. | 107.61 a.u. | 79.49 a.u. |

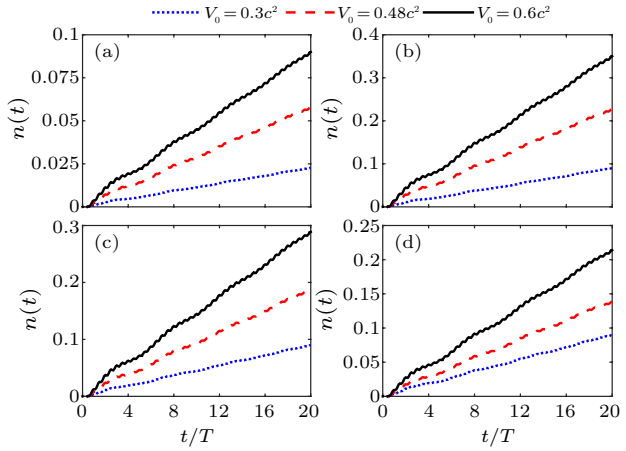



**Fig. 3.** Evolution of the number of electron–positron pairs for different distances between fields and the number of fields: (a) $d = 0$, $M = 1$, (b) $d = 0$, $M = 2$, (c) $d = W_0$, $M = 2$, and (d) $d = 2W_0$, $M = 2$. The blue dotted line, the red dashed line, and the black solid line represent $V_0 = 0.3c^2$, $0.48c^2$, and $0.6c^2$, respectively. Here, $W_0 = 3/c$ and $\omega = 2.5c^2$. The time is in units of the laser period $T = 2\pi/\omega$.

### 3.2. Pair creation's spatial dependence

In the preceding section, we investigate pair creation from multiple fields with equal distance. Additionally, we have analyzed the influence of different distance between two fields on pair creation process in this section. The two fields are partially overlapped, i.e., $d \leq W_0$. We assume that the electron–positron pairs created by the oscillating field are homogeneous in the field region considering the dipole approximation.[13–19] We first neglect the interference effects to explore the impact of overlapping extent on pair creation. Here, we introduce the reduced pair number $n'_M = n_M/W$. Because two fields completely overlapping will double the field strength, the reduced pair number of two fields $n'_2 = 4n'_1$ when $d = 0$. Sketch of the potential is presented to clearly indicate overlapped and non-overlapped regions, as shown in Fig. 4. The hypothesis of the homogeneous pair creation rate leads to five different spatial regions in the configuration. The regimes I and V are zero field area and no pairs are created there. The reduced pair number is $n'_1$ in the regions Ⅱ and Ⅳ, while the reduced pair number is $4n'_1$ in the overlapped region (Ⅲ). From Fig. 4, the total number of two fields $n_2 = (W_0 - d)n'_2 + 2dn'_1 = (4 - 2d/W_0)n_1$. Therefore, the pair number is linearly relative to the distance between two fields if we have the homogeneous creation hypothesis. However, the pair number $n_2$ has a parabolic-like relationship with the distance $d$ in our simulation results, as shown in Fig. 5. The pair creation must be inhomogeneous in space even with constant field strength, and the dipole approximation is invalid, because the characteristic length of the pair process $l_c$ is not far smaller than the laser wavelength $\lambda$.[19] Consequently, the pair creation process is space-dependent in the interaction region.

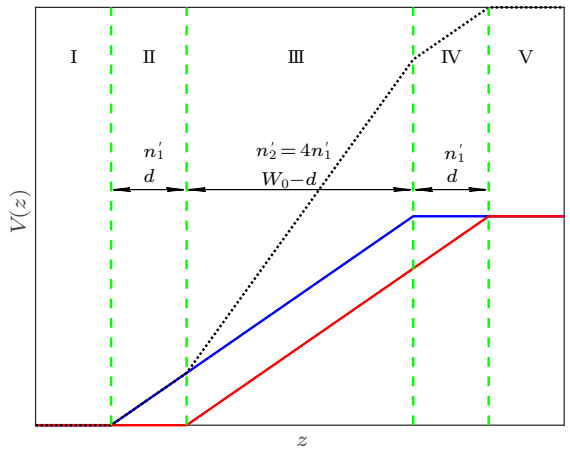



**Fig. 4.** Schematic of combined field between two fields. The blue solid and the red solid denote the left field and right field, respectively. The black dotted line denotes the combined field.

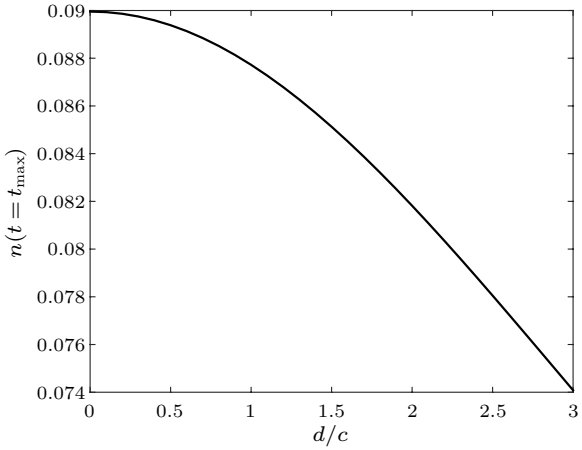



**Fig. 5.** Dependence of the created pair number on the distance between two fields. Here, $V_0 = 0.3c^2$, $W_0 = 3/c$, $\omega = 2.5c^2$, and $t_{\max} = 20T$.

To mitigate the influence of the motion of the created pairs, we evaluate the spatial distribution of pairs at time $t = T$.

As shown in Fig. 6, the spatial distribution is both Gaussian and biased, presenting the inhomogeneity of pair creation in an oscillating field.

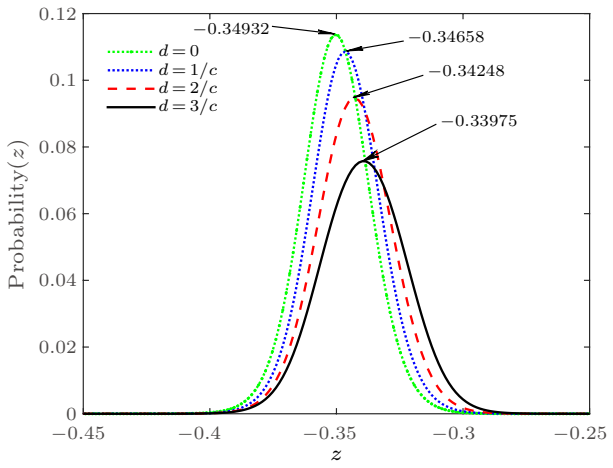



**Fig. 6.** Spatial distribution of the created pairs for different distances. The green dot-dashed line, the blue dotted line, the red dashed line, and the black solid line represent $d=0$, $d=1/c$, $d=2/c$, and $d=3/c$, respectively. Here, $V_0=0.3c^2$, $W_0=3/c$, $\omega=2.5c^2$ and $t=T$.

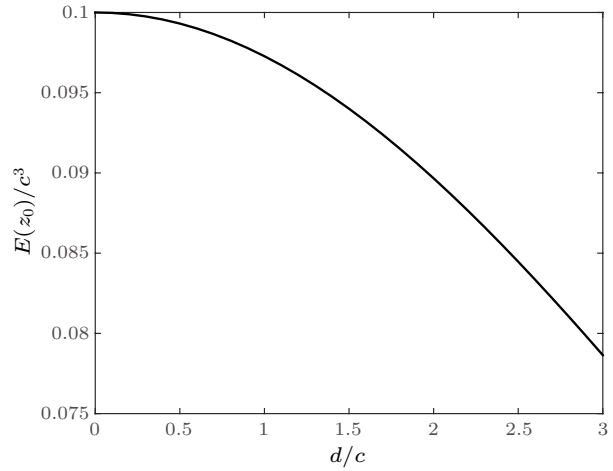



**Fig. 7.** Strength of the field at the center versus the distance between two fields. Here, $V_0=0.3c^2$ and $W_0=3/c$.

Moreover, the peak of the spatial distribution is defined by the maximum of created pairs. We find that the peak of the spatial distribution is shifted to the right with increasing the distance, as shown in Fig. 6. The displacement of the peak $\Delta z=d/2$. The peak locates at the combined field center which is at $-0.34932$, $-0.34658$, $-0.34248$, and $-0.33838$. Therefore, we can conclude that the field center is the most pair creation zone. In addition, the peak of the spatial distribution becomes smaller as the distance between two fields increases (see Fig. 6). The peak height depends deeply on the strength of field center $E_0$, which is defined by the partial derivative of the electric potential with respect to $z$ (i.e., $E_0=\partial V(z,t)/\partial z|_{z=z_0}$). With the increment of the distance between two fields, $E_0$ becomes smaller (see Fig. 7) in the reason that Sauter-like potential has a long tail with an exponential decay, and it results in the decrement of the peak height. Hence, the pairs creation process is inhomogeneous in the field region, and the electron–positron pairs are mainly created in the zone of strong strength.

## 4. Conclusion

In summary, we have realized that multiple equally spaced identical electric fields would lead to a significant electron–positron pair creation. The creation rate of pairs is directly proportional to the square of the electric field strength on a weak and rapidly altering field. In studying the process of the creation by multiple adjacent fields, we notice that the creation rate exhibits different behaviors when the fields overlap or not. The number of particle pairs created in the case of completely overlapping multiple electric fields is $M^2$ times higher than that of a single field because the total field strength is enhanced by a factor of $M$. When the fields do not overlap, the number of created pairs increases linearly with the number of fields. However, because there is mutual interference, the total number exceeds the sum of the fields alone, i.e., $M$ times of that created by a single field. The in-depth study of the above two cases demonstrates the inhomogeneous creation rate in the interaction region, and the pair creation is concentrated in the central region where the field strength is strongest. Therefore, when multiple fields exist simultaneously, whether they overlap results in the stronger field in some regions, which dominates the final number of particles created.

## Acknowledgements

This work was supported by the National Natural Science Foundation of China (Grant Nos. 11974419, 11605286, and 12204001) and the National Key R&D Program of China (Grant No. 2018YFA0404802).

## References

[1] Di Piazza A, Müller C, Hatsagortsyan K Z and Keitel C H 2012 *Rev. Mod. Phys.* **84** 1177
[2] Xie B S, Li Z L and Suo T 2017 *Matter Radiat. Extremes* **2** 225
[3] Dirac P A M 1928 *Proc. R. Soc. Lond. A* **117** 610
[4] Sauter F Z 1931 *Physik* **69** 742
[5] Heisenberg W and Euler H Z 1936 *Physik* **98** 714
[6] Schwinger J 1951 *Phys. Rev.* **82** 664
[7] Brezin E and Itzykson C 1970 *Phys. Rev. D* **2** 1191
[8] Dunne G V and Schubert C 2005 *Phys. Rev. D* **72** 105004
[9] Dunne G V, Wang Q H, Gies H and Schubert C 2006 *Phys. Rev. D* **73** 065028
[10] Schützhold R, Gies H and Dunne G 2008 *Phys. Rev. Lett.* **101** 130404
[11] Dumlu C K and Dunne G V 2011 *Phys. Rev. D* **84** 125023
[12] Schneider C, Torgrimsson G and Schützhold R 2018 *Phys. Rev. D* **98** 085009
[13] Hebenstreit F, Alkofer R, Dunne G V and Gies H 2009 *Phys. Rev. Lett.* **102** 150404
[14] Nuriman A, Xie B S, Li Z L and Sayipjamal D 2012 *Phys. Lett. B* **717** 465
[15] Abdukerim N, Li Z L and Xie B S 2013 *Phys. Lett. B* **726** 820
[16] Li Z L, Lu D, Xie B S, Fu L B, Liu J and Shen B F 2014 *Phys. Rev. D* **89** 093011
[17] Kohlfürst C, Gies H and Alkofer R 2014 *Phys. Rev. Lett.* **112** 050402

[18] Gong C, Li Z L, Xie B S and Li Y J 2020 *Phys. Rev. D* **101** 016008
[19] Ruf M, Mocken G R, Müller C, Hatsagortsyan K Z and Keitel C H 2009 *Phys. Rev. Lett.* **102** 080402
[20] Hebenstreit F Alkofer R and Gies H 2010 *Phys. Rev. D* **82** 105026
[21] Hebenstreit F, Alkofer R and Gies H 2011 *Phys. Rev. Lett.* **107** 180403
[22] Blinne A and Gies H 2014 *Phys. Rev. D* **89** 085001
[23] Li Z L, Lu D and Xie B S 2015 *Phys. Rev. D* **92** 085001
[24] Li Z L, Li Y J and Xie B S 2017 *Phys. Rev. D* **96** 076010
[25] Kohlfürst C and Alkofer R 2018 *Phys. Rev. D* **97** 036026
[26] Kohlfürst C 2019 *Phys. Rev. D* **99** 096017
[27] Li Z L, Xie B S and Li Y J 2019 *Phys. Rev. D* **100** 076018
[28] Cheng T, Su Q and Grobe R 2010 *Contemp. Phys.* **51** 315
[29] Su Q, Su W, Lv Z Q, Jiang M, Lu X, Sheng Z M and Grobe R 2012 *Phys. Rev. Lett.* **109** 253202
[30] Jiang M, Su W, Lu X, Sheng Z M, Li Y T, Li Y J, Zhang J, Grobe R and Su Q 2011 *Phys. Rev. A* **83** 053402
[31] Jiang M, Su W, Lv Z Q, Lu X, Li Y J, Grobe R and Su Q 2012 *Phys. Rev. A* **85** 033408
[32] Jiang M, Lv Q Z, Sheng Z M, Grobe R and Su Q 2013 *Phys. Rev. A* **87** 042503
[33] Tang S, Xie B S, Lu D, Wang H Y, Fu L B and Liu J 2013 *Phys. Rev. A* **88** 012106
[34] Lv Q Z, Li Y J, Grobe R and Su Q 2013 *Phys. Rev. A* **88** 033403
[35] Dong S S, Chen M, Su Q and Grobe R 2017 *Phys. Rev. A* **96** 032120
[36] Lin N S, Han L X, Jiang M and Li Y J 2018 *Acta Phys. Sin.* **67** 133401 (in Chinese)
[37] Lv Q Z, Su Q and Grobe R 2018 *Phys. Rev. Lett.* **121** 183606
[38] Lv Q Z, Dong S, Li Y T, Sheng Z M, Su Q and Grobe R 2018 *Phys. Rev. A* **97** 022515
[39] Gong C, Li Z L and Li Y J 2018 *Phys. Rev. A* **98** 043424
[40] Su Q and Grobe R 2019 *Phys. Rev. Lett.* **122** 023603
[41] Zhou X X, Li C K, Jiang M, Lin N S and Li Y J 2019 *Europhys. Lett.* **128** 10001
[42] Su D D, Li Y T, Lv Q Z and Zhang J 2020 *Phys. Rev. D* **101** 054501
[43] Gong C, Li Z L, Li Y J, Su Q and Grobe R 2020 *Phys. Rev. A* **101** 063405
[44] Zhou X X, Li C K, Jiang M, Lin N S and Li Y J 2021 *Phys. Rev. A* **103** 012229
[45] Jiang M, Zheng X R, Lin N S and Li Y J 2021 *Acta Phys. Sin.* **70** 231202 (in Chinese)
[46] Su D D, Li Y T, Su Q and Grobe R 2021 *Phys. Rev. D* **103** 074513
[47] Dumlu C K 2009 *Phys. Rev. D* **79** 065027
[48] Li Z L, Gong C and Li Y J 2021 *Phys. Rev. D* **103** 116018
[49] Janet C A P, Rajesh K B, Udhayakumar M, Jaroszewicz Z and Pillai T V S 2016 *Chin. Phys. Lett.* **33** 124206
[50] Yoon J W, Kim Y G, Choi I W, Sung J H, Lee H W, Lee S K and Nam C H 2021 *Optica* **8** 630
[51] http://www.extreme-light-infrastructure.eu/
[52] Narozhny N B, Bulanov S S, Mur V D and Popov V S 2004 *Phys. Lett. A* **330** 1
[53] Dunne G V, Gies H and Schüzhold R 2009 *Phys. Rev. D* **80** 111301
[54] Bulanov S S, Mur V D, Narozhny N B, Nees J and Popov V S 2010 *Phys. Rev. Lett.* **104** 220404
[55] Aleksandrov I A, Plunien G and Shabaev V M 2017 *Phys. Rev. D* **96** 076006
[56] Greiner W, Müller B and Rafelski J 1985 *Quantum Electrodynamics of Strong Fields* (Berlin: Springer) pp. 26–56